

Investigation of the applicability of virtual gastroscopy based on postmortem computed tomography to detect changes in the stomach, along with reports of three rare cases

Haruki Fukuda^a, Rie Sano^a, Akira Hayakawa^a, Yoichiro Takahashi^a, Takafumi Okawa^a, Rieko Kubo^a, Hiroyuki Takei^b, Sachiko Awata^c, Hiroyuki Tokue^c, Hisashi Akuzawa^d, Masahiro Yuasa^d, Yoshihiko Kominato^a

^a Department of Legal Medicine, Gunma University, Graduate School of Medicine, Maebashi 371-8511, Japan

^b Department of Radiology, Gunma University Hospital, Maebashi 371-8511, Japan

^c Department of Diagnostic Radiology & Nuclear Medicine, Gunma University, Graduate School of Medicine, Maebashi 371-8511, Japan

^d Forensic Science Laboratory of Gunma Prefectural Police Headquarter, Maebashi 371-8580, Japan

Highlights

1. We investigated the applicability of postmortem virtual gastroscopy by reviewing 295 medicolegal autopsy cases seen at our institution.
2. In four cases, virtual gastroscopy based on postmortem CT had visualized important features in the hollow space within the stomach.
3. Overall, postmortem virtual gastroscopy only rarely visualized any changes in the stomach in medicolegal autopsy cases.
4. Three cases in which postmortem virtual gastroscopy identified specific changes in the stomach wall and gastric contents are presented.

Abstract

Postmortem computed tomography is now being used more commonly for routine forensic investigation. The use of 3D reconstruction techniques including virtual gastroscopy is effective and also improves the speed of interpretation, recognition, and description of specific clinical conditions. However, it has been unclear whether postmortem virtual endoscopy could be applicable for medicolegal autopsy or whether it could complement pathological examination at autopsy. Here, we investigated the applicability of postmortem virtual gastroscopy by reviewing 295 medicolegal autopsy cases seen at our institution, and found four cases in which the technique had been able to demonstrate features corresponding to changes that were evident at autopsy. Thus, postmortem virtual gastroscopy would have only rarely been effective for visualizing any change in the stomach in such cases. In addition, we describe in detail three of those cases in which virtual gastroscopy had been able to visualize changes in the stomach, including a gastric ulcer, a polyp, and the presence of foamy fluid, which were all verified at autopsy. In those cases, virtual gastroscopy was useful for understanding features in the stomach of the deceased, which were revealed by axial images of the abdomen, to forensic pathologists who were not familiar with PMCT 2D images. Taken together, our findings suggest that postmortem virtual gastroscopy might

help facilitate clear, straightforward sharing of information about PMCT images of complex anatomical structures among radiologists and forensic pathologists, as well as non-medical professionals with a limited knowledge of anatomy and physiology.

1. Introduction

Multidetector-row computed tomography (MDCT) and specialized 3D reconstruction permit visualization of fine anatomical features that may be difficult to evaluate on the basis of axial reconstruction alone [1]. Evaluation of such detail may require the use of oblique or curved reconstructions, or more complex methods such as maximum intensity projection, minimum intensity projection, surface-shaded volume rendering, and virtual endoscopy. Postmortem computed tomography (PMCT) is now being applied commonly in routine forensic investigation [2–4], but up to now virtual endoscopy has not been used often.

Virtual endoscopy is able to evaluate anatomical structures inside body cavities and hollow viscera, thus simulating fiber optic endoscopy, offering fly-through and fly-around function based on 3D data subjected to surface or volume rendering. The term “virtual endoscopy” comprises two distinct concepts: “virtual” denotes “presentation of certain physical qualities in virtual form” while “endoscopy” involves “visualization of the interior of hollow organs”. Thus, virtual endoscopy uses CT data to display hollow viscera such as the stomach, duodenum and colon as if by optical endoscopic observation [5]. The earliest applications of virtual endoscopy were for colonoscopy, bronchoscopy, gastroscopy, cystoscopy and angiography, and more recently its range of applications has extended to labyrinthoscopy, thoracoscopy and stentoscopy. In an investigation of cause

of death, Usui et al. have used postmortem virtual colonoscopy to visualize the inner surface of a twisted sigmoid colon [6].

In clinical medicine, virtual gastroscopy has been reported to be useful as a diagnostic modality for detection of lesions such as early gastric cancer, advanced gastric cancer, gastrointestinal stromal tumor, gastric lymphoma and gastric varices [7]. It has also been reported that virtual gastroscopy can detect subtle mucosal changes and differentiate them from submucosal lesions in the same way as conventional gastroscopy [8]. In an early study to assess the applicability of virtual gastroscopy using a pig stomach, the best results were obtained with plain air insufflation [9]. Among the limitations of virtual gastroscopy, false-negative results have been reported for flat regions and in cases of inadequate insufflation, whereas false-positive results have often been due to residual feces [10]. For clinical virtual gastroscopy, patients receive water followed by ingestion of an effervescent agent to distend the stomach [11]. Thus, visualization of the whole inner surface of the stomach requires adequate insufflation and absence of food debris. In medicolegal autopsy, since food debris is often present in the deceased, it has remained unclear whether postmortem virtual gastroscopy could be applicable for investigating changes in the stomach in this setting, or whether it could complement pathological examination.

Here we investigated the applicability of virtual gastroscopy based on PMCT to detect changes in the stomach by reviewing 295 autopsy cases seen at our institution, and found four cases in which postmortem virtual gastroscopy had been able to demonstrate changes including a gastric ulcer, protruding lesions such as a polyp and submucosal tumor, and foamy fluid in the stomach. Among those four autopsy cases, we describe three of them in detail.

2. Materials and methods

2.1. PMCT. The entire body of the deceased was examined using PMCT at our University Autopsy Imaging Facility. All scans were performed using a 16-slice CT scanner (Alexion/TSX-034A, Toshiba, Japan) with a slice thickness of 0.5 mm and settings of 135 kV, 200 mAs, and 1.5 s/rot for the head, and a slice thickness of 1 mm and settings of 135 kV, 150 mAs, and 1.0 s/rot for the body in supine position. Virtual gastroscopy images were reconstructed on a CT workstation (Vincent, Fujifilm, Tokyo, Japan). The CT images were interpreted by two radiologists at the Department of Diagnostic Radiology and Nuclear Medicine who had between 7 and 10 years of experience at reviewing postmortem images.

2.2. Autopsy. The pathological examination was performed by any two of five forensic pathologists at the Department of Legal Medicine who had between one and 35 years of

experience at conducting autopsy.

2.3. Review of pathological examinations and PMCT images of the stomach.

We reviewed the results of autopsy, and the axial CT images, coronal CT images or postmortem virtual gastroscopy images of the stomach for 295 autopsy cases selected between January 2016 and June 2020. This study was approved by the Ethics Committees at Gunma University Graduate School of Medicine.

3. Results

3.1. Applicability of postmortem virtual gastroscopy to demonstrate changes in the

stomach. To investigate whether virtual gastroscopy based on postmortem computed tomography is applicable for detecting changes in the stomach, we reviewed 295 autopsy cases that had been examined between January 2016 and June 2020 after excluding any deceased younger than 20 years of age, those who had undergone gastric resection, and those with severe stomach damage due to burning or postmortem changes.

Supplementary Table 1 summarizes the various causes of death in those cases. We found 43 autopsy cases in which the stomach had changes including ulcer, polyp, cancer, submucosal tumor, mucosal erosion, foreign body, and others (Table 1). For those cases, postmortem virtual gastroscopy was attempted. Among them, postmortem virtual gastroscopy was able to demonstrate features corresponding to those changes in cases 1,

12, 19, and 37, including a gastric ulcer, protruding lesions including a gastric polyp and submucosal cyst, or foamy fluid, but was unable to visualize the changes in the stomach in the other cases. In case 19, postmortem virtual gastroscopy demonstrated a protruding mass on the greater side of the body in the stomach, but could not distinguish a polyp from a submucosal tumor. However, subsequent pathological examination demonstrated that the lesion was a submucosal cyst containing eosinophilic material.

Subsequently, we reviewed the axial CT images, coronal CT images or postmortem virtual gastroscopy images of the stomach in the 295 autopsy cases. Table 2 summarizes the locations on the inner surface that had been visualized by postmortem virtual gastroscopy in relation to whether cardiopulmonary resuscitation (CPR) had, or had not, been performed. Most of the inner surface of the stomach was observable in 22 cases, but was barely demonstrated in 118. In the remaining cases, the inner surface of the stomach was partially observable. The reasons for failure of postmortem virtual gastroscopy to demonstrate the inner stomach surface were retention of fluid, insufficient gas accumulation, and the presence of food debris (Table 3). The frequency of successful visualization of most of the inner surface, or the anterior inner surface from the fundus through the body to the antrum of the stomach, was significantly higher in deceased who had undergone CPR procedures than in those who had not, and

visualization of the inner surface was significantly more unsuccessful in deceased who had not received CPR. These results suggested that CPR including bag mask ventilation might lead to gastric air insufflation, thus aiding visualization of the stomach interior.

We categorized the 295 cases into four groups based on the results of autopsy and postmortem virtual gastroscopy: (1) Autopsy had revealed pathological changes such as ulcer and polyp in the stomach, and postmortem virtual gastroscopy had consistently visualized features corresponding to those changes. (2) Autopsy had revealed pathological changes in the stomach, but postmortem virtual gastroscopy had been unable to visualize such changes. (3) Autopsy had not revealed any pathological changes in the stomach, and postmortem virtual gastroscopy had been able to visualize the inner surface of the stomach without any changes. (4) Autopsy had not revealed any pathological changes in the stomach, and postmortem virtual gastroscopy had been unable to visualize the stomach inner surface, suggesting that observation would likely have been unsuccessful. Table 4 summarizes the numbers of cases in the individual categories. Postmortem virtual gastroscopy had revealed changes in the stomach in four (1.3%) of the 295 autopsy cases, and had visualized features corresponding to changes in the stomach revealed at autopsy in four (9.3%) of 43 autopsy cases with gastric changes. Overall, postmortem virtual gastroscopy would likely have been effective only

rarely for visualizing any change in the stomach in those medicolegal autopsy cases, with only a few exceptions such as cases 3, 12, and 37, which are presented in detail below.

3.2. Reports of cases in which postmortem virtual gastroscopy had been able to demonstrate changes in the stomach.

3.2.1. Case 1. The deceased was a man in his 80s. Dementia had impaired his daily activities, and he had required assistance from his family. However, for one week before his death, his activity had decreased to such an extent that he had been unable to go to the bathroom or feed himself. One day before death, he had fallen on the floor and struck his forehead. On the morning of the following day he was found semi-conscious on his bed, and had not eaten. In the afternoon, however, his family noticed that he had lost consciousness, and he was transferred to an emergency hospital by ambulance in a state of cardiopulmonary arrest. He did not respond to subsequent treatment and died at the hospital. A medicolegal autopsy was ordered to clarify the cause of death.

Approximately 20 hours after confirmation of death, the entire body of the deceased was examined using PMCT and interpreted as described in Materials and Methods. Axial images of the abdomen demonstrated irregularity of the mucosa in the lesser curvature side at the angle of the stomach (Figure 1A). Postmortem virtual gastroscopy revealed a gastric mucosal surface defect surrounded by a mound on the lesser curvature

side of the angle (Figure 1B). These virtual gastroscopy images were valuable for the forensic pathologists who were not familiar with PMCT 2D images because it illustrated features in the stomach of the deceased. These radiologic manifestations suggested a gastric ulcer in the stomach.

At autopsy, which was started one hour after PMCT, the body measured 157 cm and weighed 47.4 kg. External examination revealed a decrease of postmortem lividity. There were only a few traces of CPR procedures including injections, bag mask ventilation, and tracheal intubation. In the internal examination, macroscopic observation revealed a gastric ulcer with a long axis of 7 cm and a short axis of 6 cm, surrounded by a mound and converging mucosal folds, on the lesser curvature side of the angle (Figure 1C), while the edge of the ulcer was not irregular. Blood coagulation was observed in the excavated region. Consistently, 140 mL of bloody fluid was found in the stomach, and melena was evident from the small intestine to the large intestine. Reduced blood was observed in organs such as the lungs, spleen, kidneys and liver. Microscopic examination of the lesion in the stomach indicated that it was a gastric ulcer. Toxicological analysis yielded no significant findings. Therefore, it was concluded that the cause of death had been bleeding from the gastric ulcer.

3.2.2. Case 12. The deceased was a man in his 80s. He had suffered from dementia, and

his daily activities had been assisted by his family. He had often been known to stay in the bathroom for a whole day. On one occasion after he had remained in the bathroom for a day and a half, his son found him in a sitting position in the bathtub unconscious with his face submerged in the water. He was transferred to an emergency hospital by ambulance in a state of cardiopulmonary arrest, but did not respond to subsequent treatment and died at the hospital. A medicolegal autopsy was ordered to clarify the cause of death.

Approximately 64 hours after confirmation of death, the entire body of the deceased was examined using PMCT with the same protocol (or parameters) as those described in Materials and Methods. Axial images of the head demonstrated a crescent shaped mixed density area in the subdural space over the right cerebral hemisphere, and compression of the right hemisphere, suggesting chronic subdural hematoma. Axial images of the abdomen revealed extensive gas accumulation from the stomach to the ileum and a smooth well-defined mass in the stomach (Figure 2A). Moreover, a multiplanar reconstruction (MPR) image of a coronary section of the abdomen generated from multislice CT images demonstrated extensive gas accumulation from the stomach to the ileum and a similar mass in the stomach (Figure 2B). Postmortem virtual gastroscopy revealed a smooth well-defined mass without ulcer on the lesser curvature side of the

angle (Figure 2C).

At autopsy, which was started one hour after PMCT, the body measured 168 cm and weighed 57.7 kg. External examination revealed no significant findings except for a few traces of the CPR. Internal examination demonstrated frothy fluid in the airways, overinflation of the lungs, and chronic subdural hematoma (volume 130 mL) with compression of the right hemisphere. However, the brain did not show substantial atrophy. In addition, macroscopic observation demonstrated a gastric polyp with a long axis of 3.2 cm, a short axis of 3 cm and a height of 1 cm on the lesser curvature side of the angle (Figure 2D). Microscopic examination of the gastric lesion indicated a gastric adenocarcinoma. Toxicological analysis yielded no significant findings. Therefore, it was concluded that the direct cause of death had been drowning, likely ascribable to chronic subdural hematoma with compression of the right hemisphere.

3.2.3. Case 37. The deceased was a woman in her 80s. She had expressed a pessimistic view of life when seen by a doctor with her daughter on the morning of her death. In the evening, staff from a care facility visited her residence after a request from the daughter. The woman was found with a rope wound around her neck and legs, and she stated that she had attempted suicide by self-strangulation, as well as drinking three cups of dishwashing liquid (approximately 400 mL) containing 33% of hydroxyl alkyl

amine oxide, which is an amphoteric surfactant used as a foam stabilizer. She vomited several times before the ambulance service arrived. However, she flatly refused to go to hospital. After the ambulance had left her residence, she suffered vomiting and diarrhea several times while her sister took care of her. Nine hours later, she lost consciousness and was transferred to an emergency hospital by ambulance in a state of cardiopulmonary arrest. She did not respond to subsequent treatment and died at the hospital. Due to cardiopulmonary arrest, gastric lavage was not undertaken. A medicolegal autopsy was ordered to clarify the cause of death.

Approximately 7 hours after confirmation of death, the entire body of the deceased was examined using PMCT with the same protocol (and parameters) as those described in Materials and Methods. Axial images of the abdomen revealed retention of fluid in the stomach and duodenum (Figure 3A). The MPR image of a coronary section of the abdomen revealed many bubbles in the stomach (Figure 3B), and postmortem virtual gastroscopy demonstrated the presence of foam in the stomach consistent with the reported ingestion of detergent (Figure 3D). These radiologic manifestations suggested the presence of foam due to detergent in the stomach.

To examine whether CT was able to detect foam on the surface of the dishwashing liquid, the latter was vigorously mixed with water at ratios of 1:10, 1:100, 1:1000 and

1:10000 in a 50-mL tube, and the mixtures were allowed to stand overnight with the tubes tilted sideways. Naked-eye examination showed foam on the surface of the mixtures, but not on the surface of the undiluted dishwashing liquid. The aliquots were scanned by CT using a slice thickness of 0.5 mm and settings of 120 kV, 100 mAs, and 0.5 s/rot. It appeared that surface of the fluid in the mixtures was not smooth (Supplementary Figure 1A, lanes 2–5), unlike that of the undiluted dishwashing liquid (lane 1); many bubbles were apparent in the mixtures (Supplementary Figure 1B–F). Thus, CT imaging was able to reveal foam on the surface of the dishwashing liquid mixed with water.

The deceased was kept at 4–8°C in a refrigerator prior to autopsy. At autopsy, which was started approximately three days after PMCT, the body measured 162 cm and weighed 40.1 kg. External examination revealed poor skin turgor and enophthalmos, with only a few traces of the CPR. Postmortem lividity did not show a substantial change. In the internal examination, macroscopic observation revealed foamy fluid in the stomach and intestine (Figure 3E), and feces were absent from the intestinal tract. Organs including the lungs, spleen, kidneys and liver were anemic. Microscopic examination showed corrosive changes on the mucosal surface of the stomach and intestine. Toxicological analysis using liquid chromatography–ion trap tandem mass spectrometry detected alkyl amine oxide and alkyl ether sulfonate in the blood, and also

in the stomach and colon contents. Biochemistry demonstrated a sodium concentration of 139.9 mEq/L and a chloride concentration of 102.9 mEq/L in the aqueous humor. These findings suggested that the direct cause of death had been hypovolemic shock caused by vomiting and diarrhea from ingestion of the dishwashing detergent with the intention of suicide.

4. Discussion

Here we investigated the applicability of postmortem virtual gastroscopy in 295 autopsy cases, and found four cases in which this modality was able to demonstrate features corresponding to changes such as gastric ulcer, polyp, submucosal cyst, and foamy fluid in the stomach, which were found at autopsy. This suggested that postmortem virtual gastroscopy would have only rarely visualized any change in the stomach of the deceased at medicolegal autopsy effectively, with the exception of cases 1, 12, and 37, which have been presented at detail.

We also clarified that the main reasons for failure of postmortem virtual gastroscopy were the presence of fluid retention, insufficient gas accumulation, and food debris. Among the cases presented, food debris was absent due to fasting in cases 1 and 12, and had been ejected from the stomach by vomiting in case 37. Moreover, in those cases, the stomach contained much gas, likely because of bag mask ventilation during CPR.

The significant difference in gastric gas accumulation between cases where CPR had, and had not, been used (Table 2) suggested that CPR might facilitate visualization of the stomach inner surface. Therefore, this appeared to be another factor affecting visualization of the stomach interior by postmortem virtual gastroscopy, in addition to the absence of food debris or fluid. Furthermore, similarly to clinical virtual gastroscopy, scans conducted in the prone and supine positions would improve visualization of the stomach inner surface. However, further investigation based on results from more cases with pathological lesions will be required to fully assess the validity of postmortem virtual gastroscopy.

Clinical usage of virtual endoscopy was effective and also increased the speed of interpretation, recognition, and description of changes or lesions in the gastrointestinal tract or airway, as described in the literature [12–14]. Virtual gastroscopy was useful for visualizing features of complex anatomical structures in cases 1, 12, 19, and 37 for forensic pathologists who were not familiar with PMCT axial images. Thus, postmortem virtual gastroscopy might be useful for clear and straightforward sharing of information about PMCT findings in complex anatomical structures among radiologists and forensic pathologists, as well as non-medical professionals with a limited knowledge of anatomy and physiology.

5. References

1. Perandini S, Faccioli N, Zaccarella A, Re TJ, Mucelli RP. The diagnostic contribution of CT volumetric rendering techniques in routine practice. *Indian J Radiol Imaging*. 2010; 20(2): 92–97.
2. Christe A, Flach P, Ross S, Spendlove D, Bolliger S, Vock P, Thali MJ. Clinical radiology and postmortem imaging (Virtopsy) are not the same: Specific and unspecific postmortem signs. *Legal Med*. 2010;12:215–222.
3. Thali MJ, Viner MD, Brogdon BG. *Brogdon's forensic radiology*, 2nd ed. CRC Press, 2011.
4. Gotsmy WF, Ebert LC, Bollinger M, Hatch GM, Ketterer T, Thali MJ, Ruder TD. A picture is worth a thousand words – The utility of 3D visualization illustrated by a case of survived pancreatic transection. *Legal Med*. 2011;13:95–97.
5. Yamada K, Morimoto M, Kishimoto M, Wisner ER. Virtual endoscopy of dogs using multi-detector row CT. *Vet Radiol Ultrasound*. 2007;48(4):318-22.
6. Usui A, Kawasumi Y, Hosokai Y, Ishizuka Y, Ikeda T, Saito H, Funayama M. A case of fatal sigmoid volvulus visualized on postmortem radiography: The importance of image optimization with multidetector computed tomography. *Legal Med*. 2016;19:32–34.
7. Kim JH, Park SH, Hong HS, Auh YH. CT gastrography. *Abdominal Imaging*.

2005;30:509–517.

8. Furukawa K, Miyahara R, Itoh A, Ohmiya N, Hirooka Y, Mori K, Goto H. Diagnostics of the invasion depth of gastric cancer using MDCT with virtual gastroscopy: comparison with staging with endoscopic ultrasound. *AJR*. 2011;197:867–875.

9. Springer P, Dessl A, Giacomuzzi SM, Buchberger W, Stöger A, Oberwalder M, Jaschke W. Virtual computed tomography gastroscopy: a new technique. *Endoscopy*. 1997;29(7):632–4.

10. Wood BJ, Razavi P, Virtual endoscopy: A promising new technology. *Am Fam Phys* 2002;66:107–12.

11. Indrajit IK, Souza JD, Pant R, Hande PC. Virtual scopy with multidetector CT. *MJAFI*. 2006;62(1):60–63.

12. Li AE, Fishman EK. Cervical spine trauma: evaluation by multidetector CT and three-dimensional volume rendering. *Emerg Radiol*. 2003;10:34–9.

13. Salvolini L, Bichi Secchi E, Costarelli L, De Nicola M. Clinical applications of 2D and 3D CT imaging of the airways: a review. *Eur J Radiol*. 2000;34:9–25.

14. Fox LA, Vannier MW, West OC, Wilson AJ, Baran GA, Pilgram TK. Diagnostic performance of CT, MPR and 3DCT imaging in maxillofacial trauma. *Comput Med Imaging Graph*. 1995;19:385–95.

6. Figure legends

Figure 1. Gastric ulcer. A. PMCT image of an axial section of the abdomen. Arrow in the stomach indicates the direction of the view in panel B. w110 ww250. B. Postmortem virtual gastroscopy image depicting a luminal view of the stomach. The image was reconstructed by viewing the lesser curvature side of the angle from the greater curvature; a, cardia: b, fluid in the fundus: c, ulcer. The gastric ulcer, surrounded by a mound, is prominent on the lesser curvature side of the angle. C. Macroscopic findings in the stomach. The gastric ulcer was evident on the lesser curvature side of the angle. Blood coagulation was evident in the excavated region. Gastric mucosal folds were not prominent due to postmortem changes.

Figure 2. Gastric polyp. A. PMCT image of an axial section of the abdomen. Accumulation of gas is remarkable in the stomach. Arrow indicates a polyp. Window level, 30: window width, 350. B. MPR image of a coronary section of the abdomen. Arrow indicates a polyp. w130 ww350. C. Postmortem virtual gastroscopy image depicting a luminal view of the stomach. The image was reconstructed by viewing the lesser curvature side of the angle from the greater curvature; a, fundus: b, mass: c, pylorus. A smooth well-defined mass without ulcer was evident on the lesser curvature side of the angle. D. Macroscopic findings in the stomach. A gastric polyp was prominent on the

lesser curvature side of the angle. Gastric mucosal folds were not prominent due to postmortem changes.

Figure 3. Foamy fluid in the stomach. A. PMCT image of an axial section of the abdomen. Retention of fluid and accumulation of air are remarkable in the stomach. It is noteworthy that the surface of the fluid is not smooth. B. MPR image of a coronary section of the abdomen. The bubbles in the stomach are obvious. C. MPR image of a coronary section of the abdomen. Arrow in the stomach indicates the direction of the view in panel D. D. Postmortem virtual gastroscopy image depicting a luminal view of the stomach. The image was constructed by viewing the surface of the liquid from the gastric body to the fundus; a, cardia; b, fluid. Bubbles on the surface of the liquid are prominent. E. Macroscopic findings in the stomach. When the greater curvature side of the fundus was opened, foamy fluid was found in the stomach. Foam was present on the inner surface of the fundus. Gastric mucosal folds are not prominent due to postmortem changes.

Supplementary Figure 1. CT images of foam on the surface of dishwashing liquid.

The dishwashing liquid was mixed with water in a 50-mL tube, and the mixtures were left to stand overnight with the tubes sideways. Row 1 shows CT images of the undiluted dishwashing liquid, and rows 2–5 correspond to those of the dishwashing liquid diluted with water at 1:10, 1:100, 1:1000 and 1:10000, respectively. **A.** Short axis images of the liquid including the mixtures or the undiluted dishwashing liquid in the tubes. MPR images in panel B were constructed at a cross-section including the red lines, while the images in panel C were constructed at a cross-section including the yellow lines. **B.** MPR images of the surface of the liquid including the mixtures or the undiluted dishwashing liquid in the tubes. **C.** MPR images of the surface of the fluid including the mixtures or the undiluted dishwashing liquid in the tubes. **D.** Virtual endoscopic images of the surface of the liquid including the mixtures or the undiluted dishwashing liquid in the tubes. Images were constructed by viewing the surface of the liquid from the front. **E.** Virtual endoscopic images of the surface of the liquid including the mixtures or the undiluted dishwashing liquid in the tubes. Images were constructed by viewing the surface of the liquid from the front and slightly below.

Table 1. Findings in the stomach and availability of postmortem virtual gastroscopy.

Case	*Autopsy findings	†Postmortem Virtual Gastroscopy	‡Visualization					§Cause of unsuccess		
			1	2	3	4	5	fluid	gas	food debris
1	Ulcer: the lesser curvature side: size, 7 cm	+		■				■		
2	Ulcers: the antrum: size, 0.4–1.5 cm	-		■						
3	Ulcer: the lesser curvature side: size, 2 cm	-			■			■		
4	Ulcers: the lesser curvature side: size, 1.5–5 cm	-				■		■		
5	Ulcer: the lesser curvature side: size, 0.7 cm	-				■		■		
6	Ulcer: the lesser curvature side: size, 0.7 cm	-				■		■		
7	Ulcers: the fundus: size, 1.5–2 cm	-				■		■		
8	Ulcers: the fundus: size, 0.4 cm	-				■		■		
9	Ulcers: the lesser curvature side: size, 0.7 cm	-				■		■		
10	Ulcer: the antrum: size, 1.5 cm	-				■		■		
12	Polyp: the lesser curvature side, size, 3.2 cm	+	■							
13	Polyp: the lesser curvature side: size, 0.4 cm	-		■				■		
14	Polyps: the lesser curvature side: size, 0.7 cm	-		■				■		■
15	Polyp: the lesser curvature side: size, 1.5 cm	-					■	■		
16	Polyps: the lesser curvature side: size, 0.7 cm	-					■	■		■
17	Polyp: the lesser curvature side: size, 0.7 cm	-					■	■		■
18	Advanced cancer: the fundus: size, 6 cm	-				■		■		
19	Advanced cancer: the antrum: size, 8 cm	-				■		■		
19	Submucosal tumor: the greater curvature side: size, 1.5 cm	+		■						■
20	Submucosal tumor, the antrum: size, 0.7 cm	-			■			■		
21	Mucosal erosion	-		■				■		
22	Mucosal erosion	-		■				■		
23	*Mucosal erosion	-		■				■		
24	*Mucosal erosion	-		■				■		
25	*Mucosal erosion	-		■				■		
26	*Mucosal erosion	-			■			■		
27	*Mucosal erosion	-			■			■		
28	*Mucosal erosion	-			■			■		
29	*Mucosal erosion	-			■			■		
30	Mucosal erosion	-			■			■		
31	*Mucosal erosion	-			■			■		
32	Mucosal erosion	-			■			■		
33	Mucosal erosion	-			■			■		
34	*Mucosal erosion	-			■			■		
35	Mucosal lacerations: the lesser curvature side: size, 2.5–3 cm	-		■				■		
36	Disruption: the fundus: size, 7 cm	-			■			■		
37	Detergent	+		■				■		
38	*Sand particles	-			■			■		
39	*Sand particles, leaves	-					■	■		
40	*Sand particles, leaves	-					■	■		
41	*Sand particles	-					■	■		
42	*Sand particles	-					■	■		
43	*Tablet	-					■	■		■

*Autopsy findings included a pathological lesion or change, its location, and its size. The finding “*Mucosal erosion” was observed in cases of exposure to cold, and the finding “*Sand particle” or “*Tablet” was observed in cases of drowning.

†“+” denotes capability of postmortem virtual endoscopy to visualize a pathological change in the stomach: “-” denotes incapability of postmortem virtual endoscopy to visualize a pathological change in the stomach.

‡Filled box denotes the location of the inner surface visualized by postmortem virtual gastroscopy: 1, Most of the inner surface of the stomach: 2, Anterior inner surface of the fundus through the body to the antrum: 3, Anterior or whole inner surface of the fundus: 4, Anterior or whole inner surface of the antrum: 5, No part of the stomach inner surface.

§Filled box denotes the main reason why postmortem virtual gastroscopy was unable to visualize the inner surface of the stomach.

“Gas” denotes “insufficient gas accumulation”.

Table 2. Locations of air in the stomach in cases where it was possible to observe the inner surface using postmortem virtual gastroscopy in the presence or absence of CPR.

*Locations of the stomach	Total	Presence	Absence	†Statistics
Most inner surface of the stomach	22	16	6	p <0.01
Anterior inner surface from the fundus through the body to the antrum of the stomach	66	37	29	p <0.01
Anterior inner surface from the fundus to the body of the stomach	5	2	3	-
Anterior or whole inner surface in the fundus of the stomach	49	15	34	-
Anterior inner surface in the body of the stomach	1	0	1	-
Anterior or whole inner surface in the antrum of the stomach	34	10	24	-
None of inner surface of the stomach	118	34	84	p <0.01
Total	295	114	181	

*Location of air in the stomach was determined by axial CT image, coronal CT image or postmortem virtual gastroscopy image in individual cases.

†Significant difference between the presence and absence of CPR by Pearson's chi-squared test with Yates' correction (p<0.01).

Table 3. Main reasons for failure to observe the inner surface by postmortem virtual gastroscopy.

*Main reason	Number	Ratio (%)
Retention of fluid	118	43.0
Insufficient gas accumulation	91	33.2
Food debris	64	23.7
Total	274	100

*The main reason why the inner surface could not be observed by postmortem virtual gastroscopy was assumed on the basis of autopsy findings, axial CT imaging, coronal CT imaging or postmortem virtual gastroscopy imaging, although fluid retention, insufficient gas accumulation, or food debris was present in many cases.

Table 4. Summary of the availability of postmortem virtual gastroscopy for detection of changes in the stomach.

		*Postmortem virtual gastroscopy	
		Successful	Unsuccessful
Pathological changes in the stomach found at autopsy	Presence	†4	39
	Absence	21	231

*A verdict of successful or unsuccessful was made according to whether features corresponding to the changes found at autopsy, or on the inner surface of the stomach, were observed successfully.

†Postmortem virtual gastroscopy demonstrated features corresponding to the changes found at autopsy in three cases where the inner surface of the stomach was partially visualized.

Figure 1

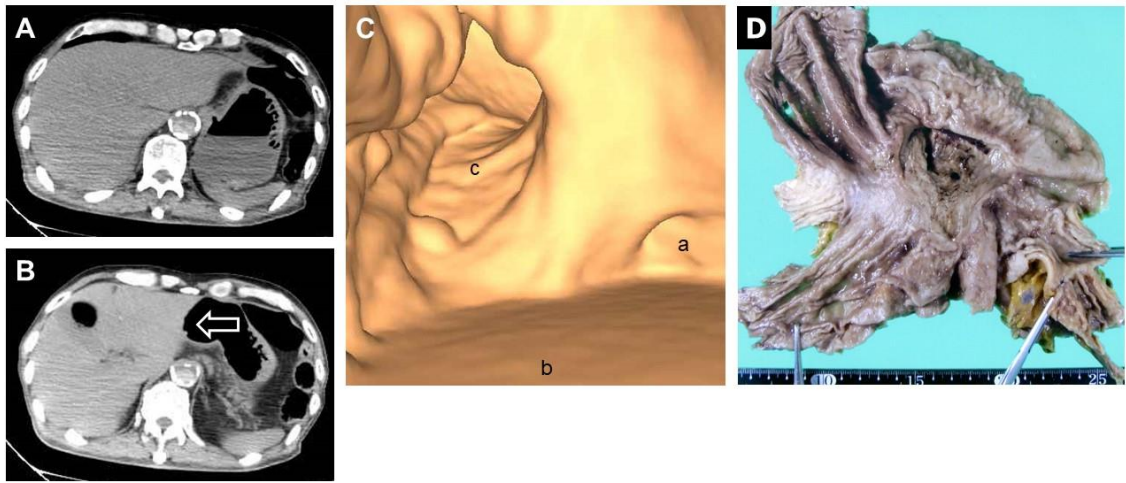


Figure 2

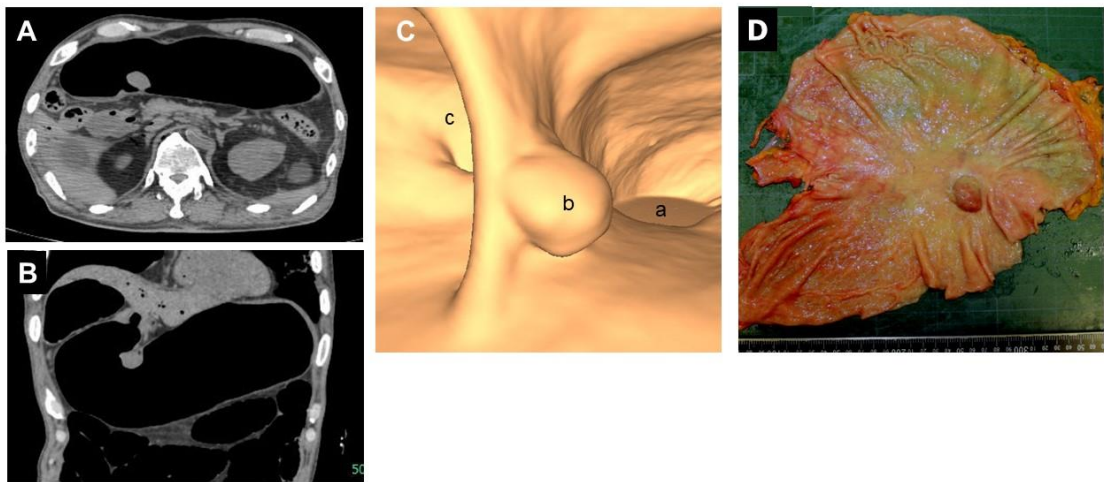
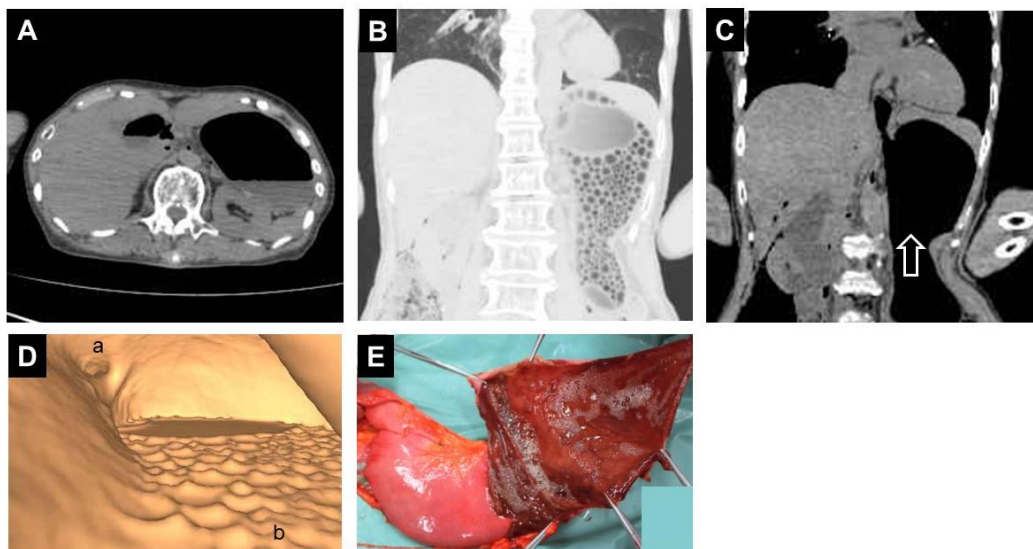
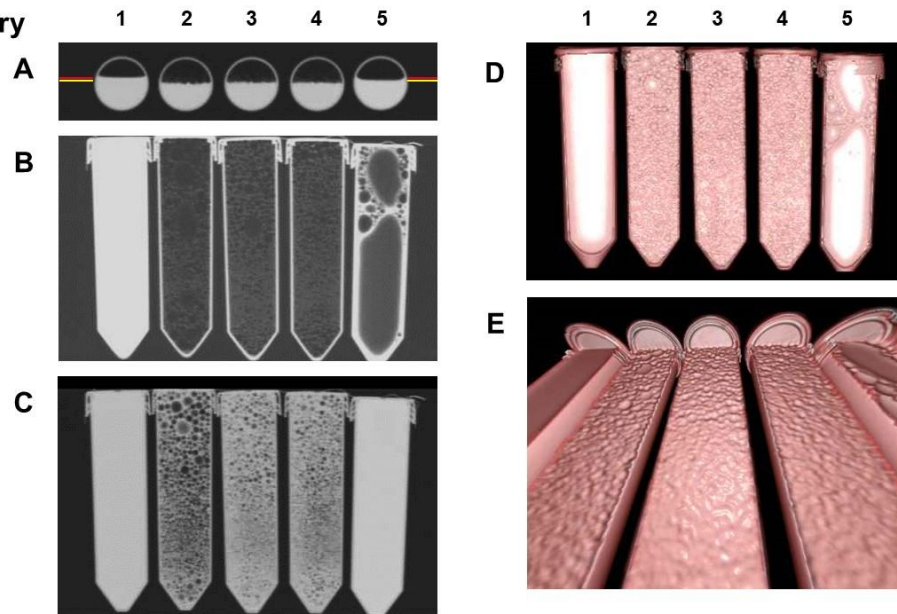


Figure 3



**Supplementary
Figure 1**



Supplementary Table 1. Classification of causes of death in the 295 cases.

Causes of death	Number	Ratio (%)
Disease	48	16.3
Mechanical injury	89	30.2
Asphyxia	13	4.4
Drowning	40	13.6
Abnormal circumstance	25	8.5
Poisoning	26	8.8
Not determined	54	18.3